scientific reports

OPEN

Design and development of a graphene-based MIMO antenna for smart multi-band sub-6 GHz 5G wearable communication applications

A. J. A. Al-Gburi[1], N. J. Mohammed[2]✉, Tale Saeidi[3], Nurhayati Nurhayati[4] & M. M. Ismail[5]✉

Traditional copper-based planar antennas have traditional disadvantages for wearable applications because of poor flexibility, deteriorated signal under deformation, expensive and environmental problems. To solve these issues, graphene has been proposed as a radiating material with high electrical conductivity, great flexibility, and the possibility of being printed on low-cost textile/paper substrates. In this study, graphene was used as a conductive material in an a two-port MIMO antenna for wearable smart communication. The graphene MIMO wearable antenna is printed on Jeans with a dielectric constant of 1.67, and an overall dimension of 35 × 55 mm³. The antenna operates in a multiband mode within the 5G sub-6 GHz spectrum, covering two distinct frequency ranges of 3.1–4.3 GHz and 4.9–6.0 GHz. This makes it a strong candidate for wearable 5G sub-6 GHz terminals, body-centric wireless communication systems, and short-range WLAN/ISM-based smart wearable devices. In addition, higher-order resonant bands at 8.25–9.4 GHz and 10.82–14.4 GHz are observed, indicating that the proposed design inherently exhibits wideband characteristics in the X-band region. The graphene is highly electrically conductive being 4.02×10^5 S/m. The SAR analysis was carried out for the entire bandwidth, and it can be seen that energy absorption tends to be more restricted by increasing the skin depth (SC and OC) with higher frequency because of the dependence of dielectric properties on frequency. The maximum measured SARs are quite low below the ICNIRP safety limits 0.84 W/kg averaged over 10 g of tissue at an input power of 0.5 W, and hence it indicates that the proposed graphene-based MIMO configuration is a suitable solution for long-term wearable applications as it does not impose any health threats to the user.

Keywords Graphene, MIMO antenna, Wearable, Sub-6 GHz 5G, Multi-band, X-band, Electrical conductivity, Specific absorption rate (SAR)

With the rapid progress in wireless communication technology, flexible and high-performance RF antennas are increasingly required in wearable devices[1–8]. These new platforms require conductive materials that can maintain stable electrical characteristics even under mechanical deformation, such as bending, twisting, and stretching. To increase the flexibility of antennas, much effort has been made to decrease the thickness of metal conductors[9–11], because the flexural rigidity of a metal is directly proportional to its thickness[12]. Thus, thinner metal films have better flexibility and are more compatible with flexible substrates.

To address this constraint, graphene has been considered a potential substitute material for flexible and stretchable electronics owing to its high electrical conductivity, excellent mechanical properties, and outstanding

[1] Strategic Research Institute (SRI), Asia Pacific University (APU), Jalan Teknologi 5, Taman Teknologi Malaysia, 57000 Kuala Lumpur, Malaysia. [2]Department of Applied Physics, Faculty of Science and Technology, Universiti Kebangsaan Malaysia, Bangi 43600, Selangor, Malaysia. [3]WiSAR Lab, Atlantic Technological University (ATU), Letterkenny F92 FC93, Ireland. [4]Department of Electrical Engineering, Universitas Negeri Surabaya, Surabaya 60231, Indonesia. [5] Fakulti Teknologi dan Kejuruteraan Elektronik dan Komputer (FTKEK), Universiti Teknikal Malaysia Melaka (UTeM), Jalan Hang Tuah Jaya, 76100 Durian Tunggal, Melaka, Malaysia. ✉email: nabaa@ukm.edu.my; muzafar@utem.edu.my

flexibility[13,14]. Second, the bonded- and dangling-bond-free surface in graphene membranes is better desertified with other materials, including metals and polymers, which helps strengthen robustness and durability[15]. Furthermore, the skin-effect characteristics of graphene are negligible, which is highly desirable for high-frequency wireless communication applications.

Recently, wearable antennas using conductive materials and flexible supports have been developed. Zhou et al.[16]. reported an eco-friendly screen-printed graphene ink for metal-free RFID antennas with high conductivity and far-field reading distance, while Ibanez-Labiano et al.[17]. developed CVD-graphene flexible textile antennas for 3–9 GHz, which also exhibited wideband characteristics under bending and on-body loading.

Douhi et al.[18]. proposed a flexible wideband antenna on a PVDF-HFP/BCZT composite substrate with a good efficiency and SAR-compliant performance, highlighting the role of high-performance flexible dielectrics in wearable RF designs.

On the substrate side, Gil and Fernández-García[19] introduced an embroidered-jeans-based PIFA that satisfies 2.45 GHz WBAN SAR limits, while Mulkalla et al.[20] and Chen et al.[21] demonstrated compact jeans-substrate patches and UWB antennas that maintain good gain and matching under bending, confirming denim as a low-ε_r, low-loss textile substrate. Aydın[22] showed that 3D-printed graphene bowtie microstrip antennas can achieve ultra-wide bandwidth and high gain, and Shyni et al.[18] reported a simple bowtie jean antenna with a strong ISM-band performance. Together, these studies[16–23] motivated the present design of a printed graphene MIMO antenna for smart wearable communication.

Recent studies have advanced the use of conductive materials and flexible substrates in wearable antennas. Zhou et al.[16]. developed a sustainable screen-printed graphene ink that enables metal-free RFID antennas with high conductivity and reliable far-field sensing, whereas Ibanez-Labiano et al.[17]. demonstrated CVD-graphene soft textile antennas operating at 3–9 GHz that retain wideband performance under bending and on-body loading. Douhi et al.[18]. further highlighted the role of flexible dielectrics by proposing a wideband wearable antenna based on a PVDF-HFP/BCZT composite substrate with a good efficiency and SAR-compliant behavior.

On the substrate side, Gil and Fernández-García[19] introduced an embroidered-jeans-based PIFA satisfying WBAN SAR limits of 2.45 GHz. Subsequent studies confirmed that denim is a suitable wearable substrate, including compact patches and UWB antennas on jeans, as reported by Chen et al.[20]., Mulkalla et al.[21]., and Chen et al.[22]., who demonstrated stable impedance matching, sufficient gain, and robustness under bending. In parallel, Aydın[23] showed that graphene-based bowtie microstrip antennas fabricated via additive manufacturing can achieve an ultrawide bandwidth and high gain. Collectively, these studies[16–23] motivated the present design of a printed graphene MIMO antenna on a denim substrate for smart wearable communication systems.

The main contributions and novelties of this work can be summarized as follows:

- Design and realization of a fully printed graphene-based two-port MIMO antenna on a real denim (jeans) textile substrate, addressing flexibility, durability, and environmental sustainability challenges of metallic wearable antennas.
- Targeted multiband operation covering the 5G sub-6 GHz spectrum (3.1–4.3 GHz and 5.9–6.0 GHz), the 8.25–9.4 GHz band, and the 10.28–14.4 GHz band, achieved within a compact wearable form factor without the need for additional tuning or reconfigurable circuits.
- Experimental validation of MIMO performance on a textile platform, including impedance matching, isolation, and radiation characteristics under body-centric conditions.
- Comprehensive SAR assessment over the entire operational bandwidth using multilayer human tissue models, demonstrating compliance with ICNIRP safety limits and confirming suitability for long-term wearable use.

To the best of our knowledge, this work is the first to report a graphene-based MIMO antenna printed on jeans textiles for smart multiband 5G wearable communication applications. This paper presents the design and development of a two-port graphene MIMO wearable antenna operating in a multiband manner within the 5G sub-6 GHz spectrum. The proposed antenna is fabricated on a Jeans material with a relative permittivity of 1.67, a loss tangent of 0.025, and a thickness of 0.5 mm. The graphene radiating element exhibits a high electrical conductivity of 4.02×10^5 S/m. In addition, a comprehensive SAR analysis was performed using multilayer human tissue models comprising the skin, fat, and muscle, confirming that the antenna satisfies international exposure limits and is suitable for safe on-body wearable applications.

Design and preparation process of the graphene antenna geometry

Graphene-based MIMO antenna geometry

The textured graphene-based MIMO wearable antenna was fabric-printed on a demin textile (jeans), which was chosen for its flexibility and body-focused age cent wireless applications. The substrate has a relative permittivity (εr) of 1.67, loss tangent ($tan\delta$) of 0.025 mm and thickness of 0.5 mm, which ensures both mechanical robustness and good electromagnetic performance for wearable antenna integration. A graphene MIMO antenna was designed using the CST suite.

The parametric study begins with the conventional circular patch antenna shown in Fig. 1(a). This configuration exhibits a wideband impedance response extending from approximately 3.35 to 15 GHz. Although such wideband behavior may be attractive for broadband systems, it does not satisfy the objective of this work, which is to achieve controlled multiband operation with a strong resonance around 3.5 GHz for 5G sub-6 GHz applications, together with additional bands suitable for higher-frequency services such as X-band.

To introduce controlled multiband characteristics, the circular radiator is modified into a ring-shaped patch, as illustrated in Fig. 1(b). This structural modification alters the surface current distribution and increases the effective electrical length of the radiator, leading to the excitation of multiple resonant modes. As a result, the

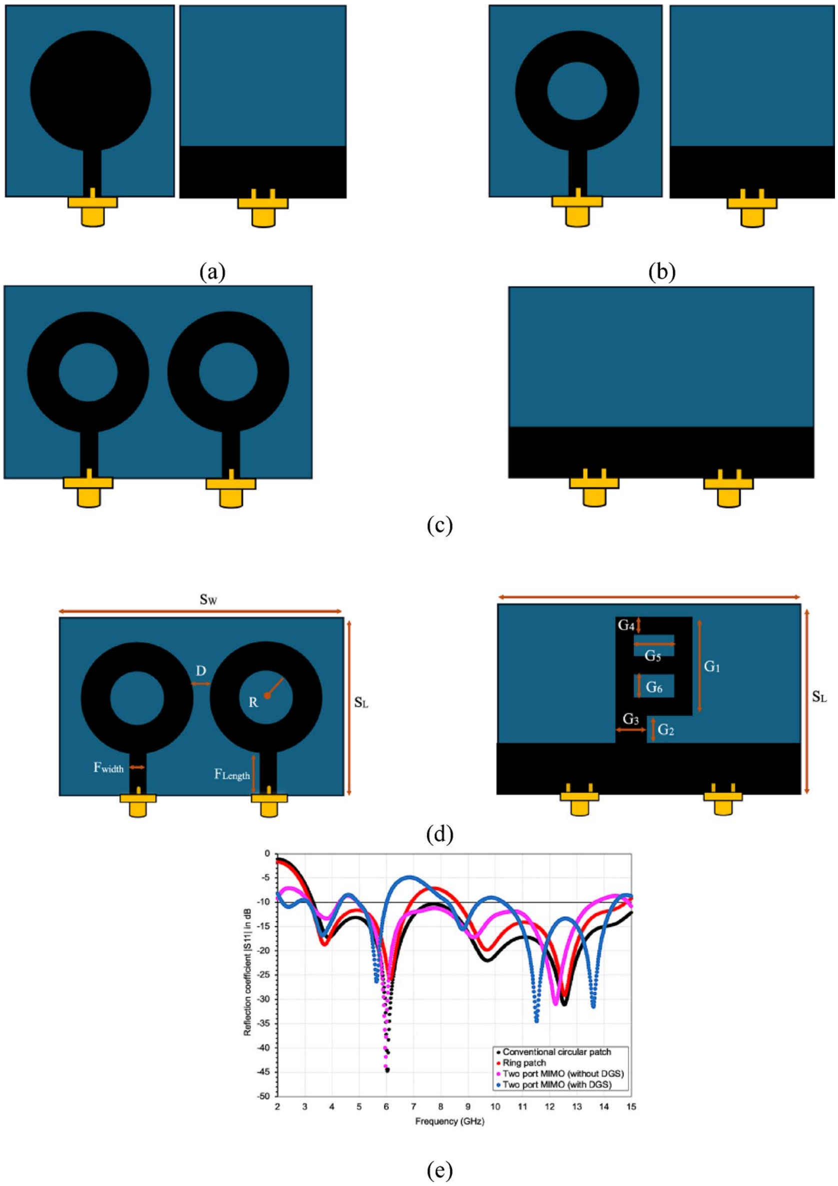

Fig. 1. Parametric study of the proposed graphene-based two-port MIMO antenna. **(a)** Conventional circular patch, **(b)** ring patch, **(c)** two-port MIMO antenna without DGS, **(d)** geometry of two-port MIMO antenna with DGS, and **(e)** reflection coefficient $|S_{11}|$ performance for all design stages.

antenna exhibits two operating bands: the first spanning approximately 3.2 to 6.9 GHz, and the second extending from 4.94 to 13.7 GHz, indicating a clear transition from wideband to multiband behavior.

The ring radiator is then extended to a two-port MIMO configuration, as shown in Fig. 1(c). In this case, the graphene-based MIMO antenna demonstrates more clearly defined multiband operation, with a first band from 3.148 to 4.25 GHz and a second band from 4.94 to 13.7 GHz. The introduction of the MIMO configuration modifies the input impedance due to mutual coupling between the two radiating elements, which reshapes and shifts the resonant modes compared with the single-element ring antenna.

Finally, a defected ground structure (DGS) in the form of a figure-of-eight (8-shaped) slot, as shown in Fig. 1(d), is introduced to improve isolation between the MIMO elements and to further enhance impedance matching. With the inclusion of the DGS, the proposed graphene-based MIMO antenna achieves a well-defined and stable multiband response. The first operating band extends from 3.1 to 4.3 GHz, with an $|S_{11}|$ value of approximately − 16 dB at 3.5 GHz, compared with about − 12.5 dB for the MIMO antenna without the defected ground structure (DGS). The second band spans 4.9 to 6.0 GHz, fully covering the 5G sub-6 GHz spectrum, and exhibits a minimum $|S_{11}|$ of − 26.33 dB at 5.64 GHz. In addition, an intermediate operating band from 8.25 to 9.4 GHz is also achieved. Furthermore, a higher-frequency band extending from 10.28 to 14.4 GHz shows excellent impedance matching, with a minimum $|S_{11}|$ of − 37.7 dB at 12.9 GHz, making the antenna suitable for X-band applications. A comparison of the S_{11} responses for all design stages is presented in Fig. 1(e).

These results confirm that the incorporation of the DGS plays a critical role in enhancing impedance matching, suppressing undesired coupling, and stabilizing the multiband performance of the proposed antenna.

The feed-line dimensions are carefully designed to ensure efficient excitation of the ring-shaped graphene radiators, while the inter-element spacing and ground-plane defects are optimized to achieve acceptable MIMO isolation. Overall, the integration of graphene as a conductive material, a low-profile textile substrate, ring-shaped radiators, and an 8-shaped DGS results in a compact, flexible, and multiband MIMO antenna suitable for wearable 5G sub-6 GHz and X-band communication applications. The detailed geometric parameters of the proposed antenna are summarized in Table 1, including the substrate dimensions, ring radiator geometry, feed-line characteristics, and DGS dimensions, which are optimized to realize the desired multiband operation with good impedance matching and MIMO isolation performance.

Graphene MIMO antenna preparation process

Graphene was selected as the radiating material in this study due to its favorable balance between electrical conductivity, mechanical flexibility, and fabrication compatibility for wearable applications. Compared with MWCNT-based composites, graphene provides higher and more stable conductivity with reduced ohmic losses at sub-6 GHz frequencies. In contrast to conductive fabrics, graphene enables accurate patterning and repeatable electrical properties without issues related to anisotropy or material degradation. While copper exhibits superior conductivity, its limited flexibility, susceptibility to fatigue and oxidation, and environmental concerns restrict its long-term use in wearable systems. These advantages make graphene particularly suitable for compact, multiband MIMO wearable antennas targeting 5G applications.

A prototype of the MIMO wearable antenna, developed in graphene, was fabricated using a silk screen-printing technique that is highly precise, repeatable, and compatible with textile substrates. The entire preparation process is shown in Figs. 2(a–i).

The design of the antenna layout (using CorelDraw) begins by drawing the optimized MIMO geometry dimensions, as provided in Table 1. The final design was printed on a transparent film that was used as the screen template (Fig. 2(a)).

Concurrently, a conductive material was fabricated using a commercial graphene ink, as shown in Fig. 2(b). Further conditioning and pre-treatment were carried out to give the inks a homogeneous dispersion together with a suitable viscosity for screen printing (Fig. 2(c)).

This photosensitive emulsion was then coated evenly on a silk screen and left to dry in a dark room to prevent premature exposure did not occur. The antenna layout film was then carefully placed on top of the screen (over the coated part) and exposed to ultraviolet (UV) light. Upon exposure, the emulsion was solidified (or "hardened") in areas not covered by the patterns of antenna; where the film was left unexposed, it remained soft and could be washed away with water to produce an accurate antenna stencil on the screen mesh (Fig. 2(d)).

The preformed silk screen was subsequently placed onto the jeans textile substrate owing to its flexibility, low dielectric properties, and wearable applications (Fig. 2(e)). Graphene printing ink was squeegeed onto the screen and then transferred to a Jeans Substrate. Controlled squeegee pressure provides uniform thickness and realistic reproduction of antenna geometry for proper conductivity and dimensions. The screen-printing process is illustrated in Fig. 2(f).

Once printed, the antenna was cured and dried using a heat press machine (Fig. 2(g)). The applied temperature and pressure conditions also helped to increase the ink-to-textile interface adhesion, promote the electrical conductive bond, and strengthen the mechanical properties such as flexibility of the antennas, resulting in good performance even when bent or worn on the human body.

Finally, SMA connectors were soldered on the antenna feed lines to ensure a good RF interface for measurements and system integration. Good soldering reduces the contact resistance for stable signal transmission. The fabricated graphene MIMO wearable antenna is illustrated in Fig. 2(h), and the back view that exposes the defective ground structure is shown in Fig. 2(i), completing the fabrication process.

Graphen antenna parameters	Calculation in mm
S_W	55
S_L	35
R	10.5
F_{width}	3.0
F_{length}	9.6
D	8.2
G_1	18
G_2	5.9
G_3	5.5
G_4	3.0
G_5	7.0
G_6	4.5

Table 1. Optimized geometrical variables of the suggested graphene-based MIMO antenna.

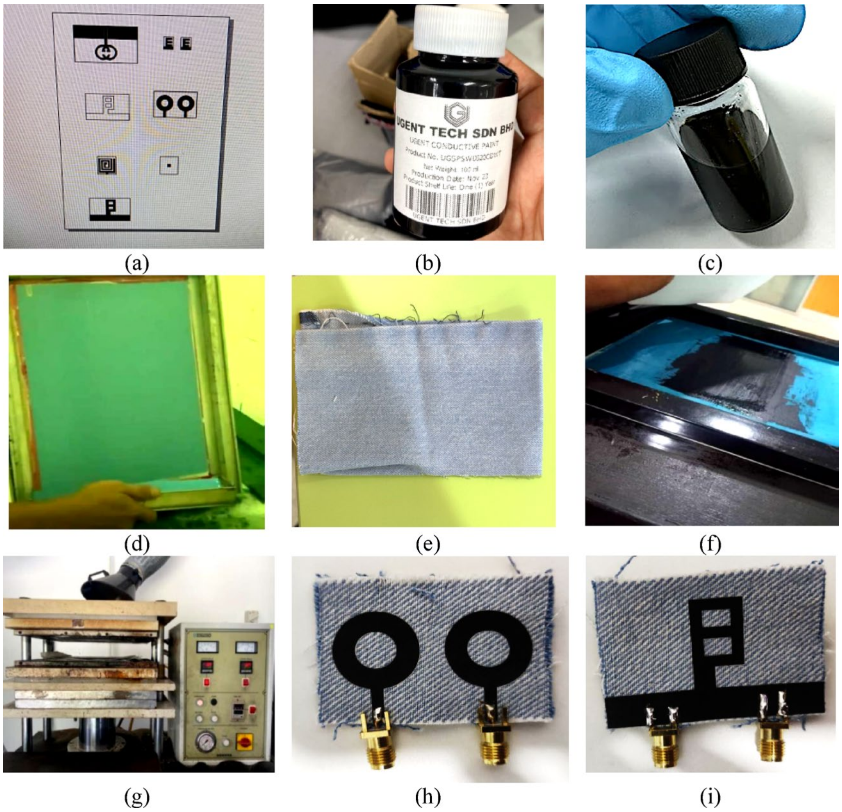

Fig. 2. Preparation and fabrication process of the graphene-based MIMO antenna on textile substrate.

Results, analysis, and discussion
Performance characterization of the graphene MIMO antenna
The simulated and measured S-parameters of the proposed graphene-based MIMO antenna are shown in Fig. 3(a). Four main resonant frequencies are observed at approximately 3.5, 5.64, 8.4 and 12.9 GHz, with corresponding simulated reflection coefficients of − 16 dB, − 26.33 dB, − 14.1 dB, and − 37.7 dB, respectively. These resonances originate from the multiple effective current paths introduced by the ring-shaped graphene radiators and the defected ground structure (DGS). Owing to the close spacing of these resonant modes, they partially merge, resulting in a broad impedance bandwidth where $|S_{11}| < -10$ dB over an extended frequency range.

At these resonant frequencies, the transmission coefficient $|S_{21}|$ remains well below − 15 dB across the operating bands, indicating good isolation and low mutual coupling between the two radiating elements. This confirms that the DGS is effective not only in generating additional resonant modes, but also in suppressing surface-current coupling paths on the ground plane, which is particularly important for wearable MIMO antennas where body proximity and bending can otherwise increase coupling. The measured S-parameter results closely follow the simulated trends, with minor discrepancies attributed to uncertainties in textile dielectric properties, non-uniform substrate thickness, imperfections in graphene ink printing, and parasitic effects introduced by SMA connectors and feeding transitions.

The impact of the resonant modes on MIMO performance is further evaluated through the envelope correlation coefficient (ECC), as shown in Fig. 3(b). Despite the presence of multiple resonances, the ECC remains very low across the entire frequency range, with a maximum value below 0.023 and values close to or below 0.01 over most of the band. These ECC values are significantly lower than the commonly accepted thresholds of 0.1 and 0.05, confirming that the excitation of multiple resonant modes does not increase correlation between antenna elements. Instead, it enables effective pattern diversity and stable MIMO operation, demonstrating the suitability of the proposed antenna for 5G sub-6 GHz and extended-band wearable communication systems.

The DG performance of the CRLH coupled-line MIMO antenna is depicted in Fig. 3(c). The diversity gain maintained a value close to the ideal value (10 dB) over all frequency ranges, confirming excellent diversity behavior. Quantitatively, the DG is ranging between approximately 9.88 dB and 10.01 dB with little up-down dips at approximately 2.8 GHz and 7.3 GHz, whereas the DG is still higher than approximately 9.9 dB. These small degradations were consistent with the regions of resonance and rapid impedance changes but did not have much impact on the general diversity performance. The small ECC in Fig. 3(b) proves the good performance of the proposed antenna for robust MIMO diversity at wearable 5G sub-6 GHz and extended-band.

The MEG performance of the proposed graphene-based MIMO antenna is illustrated in Fig. 3(d). The MEG remained relatively flat within the entire frequency range and had a value of roughly − 3.0 dB for both antenna

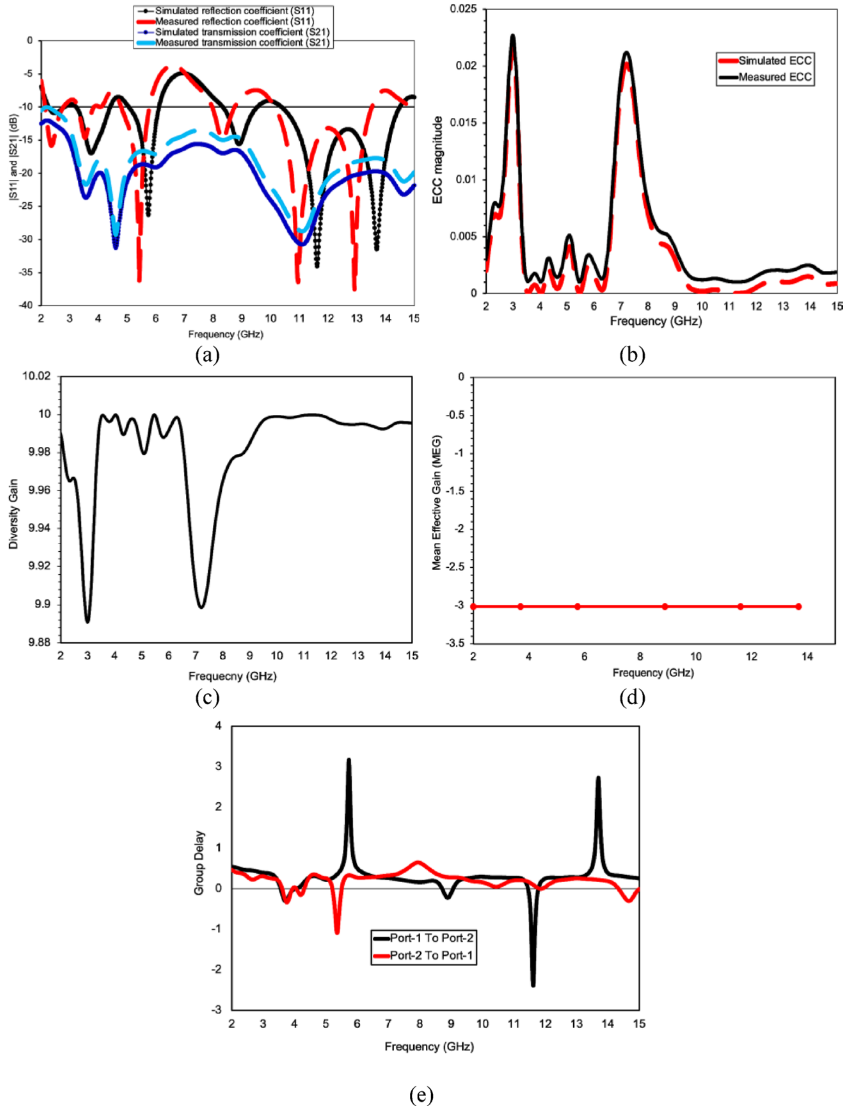

Fig. 3. Performance characterization of the proposed graphene-based MIMO antenna: **(a)** simulated and measured $|S_{11}|$ and $|S_{21}|$; **(b)** ECC; **(c)** DG; **(d)** MEG; and **(e)** group delay.

ports. The MEG variation was very small (± 0.05 dB), demonstrating very good power splitting among the mean line elements. Interestingly, no degradation in the MEG was detected at any of the five resonant frequencies, indicating that the multi-resonant operation does not compromise the power balance. This stable and symmetric MEG response is essential for robust MIMO systems, indicating that the designed antenna will be an appropriate choice for 5G sub-6 GHz and extended-band communication wearable applications.

Figure 3(e) shows the group-delay responses for the graphene-based MIMO antenna structure for two transmission paths: Port-1 to Port-2 and Port-2 to Port-1. Over most of the operation frequency, the group delay flatness is kept stable and closes around 0–0.5 ns, with low signal distortion (good time-domain envelope profile). In the Port-1 to Port-2 path, there also appear some localized peaks at around + 3.1 ns about 6.0 GHz and + 2.6 ns near 13.8 GHz, as well as a negative dip up to − 2.6 ns around 11.8 GHz are also obtained for comparison purpose. Pulsed microwave measurement. These properties are the result of the strong resonant modes and fast phase transmutations. As opposed to this, the Port-2 to Port-1 path deviates more, ranging from around + 0.09 ns to 3.2 ns (peak-to-peak) in positive offsets from the shortest time advance − 1.18 ns found at about 6 GHz below or above it's peak value. More importantly, such fluctuations are restricted within narrow frequency bands, and the overall group delay is flat across this band (as well as the entire span of interest), verifying that multi-resonant operation does not impose excessive time-domain distortion. The reliability and asymmetry of the signal transmission between the antenna ports allow an e-coat for broadband wearable MIMO communication.

In addition to the targeted sub-6 GHz operating bands, the proposed antenna exhibits higher-order resonances at approximately 12.9 GHz, which arise from multiple effective current paths introduced by the ring-shaped graphene radiators and the defected ground structure. Although these resonances highlight the inherent multiresonant behavior of the proposed design, the primary focus of this work remains on wearable and body-centric communication within the 5G sub-6 GHz spectrum, where tissue losses are comparatively lower and regulatory standards are well established.

At higher frequencies, electromagnetic wave penetration into biological tissues is reduced, leading to increased attenuation; therefore, these higher-order resonances are not emphasized as primary wearable communication bands in this study. Instead, they may be considered beneficial for off-body, short-range, or sensing-related applications, or as optional operational modes when the antenna is used away from direct body contact. If required, these higher-frequency modes can also be suppressed or controlled through additional filtering or structural optimization, depending on the intended application.

Consequently, the analysis and validation presented in this work—particularly the SAR evaluation, MIMO performance, and on-body assessment—are intentionally concentrated on the sub-6 GHz bands, which represent the most relevant and practical frequency range for wearable 5G systems.

SAR evaluation of the graphene-based MIMO antenna for wearable use

To study the on-body performance and compliance with electromagnetic exposure limits, the SAR of the MIMO antenna was calculated using anatomically based human tissue phantoms within CST Studio Suite. As illustrated in Fig. 4, two different phantom models were used, which represent typical practical wearable-use cases.

Phantom modeling and tissue properties

On-body performance was tested and electromagnetic exposure limits were compared to assess compliance using two anatomically realistic phantom models to represent realistic wearable use. We simulated two models: (a) a planar multi-layer chest phantom, for an average human torso cross-section, in which three homogenous layers—skin (1.5 mm), fat (3 mm) and muscle that comprises most of the structure surface area (50 mm thick layer) —constitute a $150 \times 170 \times 49$ mm box. In addition, to assess performance in a realistic environment, a second heterogeneous cylindrical phantom was simulated to drape the typical natural curve and internal tissue composition of the human body. In all of the simulations, the graphene-based MIMO antenna structure was placed on top of the phantoms with no air gap, as would have been done for placing this type of antenna into real on-body scenarios. The interaction between the EM fields and these layers is characterized by the basic SAR equation[24]:

$$SAR = \frac{\sigma |E|^2}{2\rho} \tag{1}$$

where σ is the electrical conductivity of the tissue (S/m), |E| is the maximum magnitude of the induced electric fields (V/m) and indicates the mass density of the tissues (kg/m^3). The mass densities (ρ) of the skin, fat, and muscle were set to 1100, 910, and1040 kg/m^3 respectively. Table 2 (Fig. 4). The frequency dependent dielectric properties (ϵ_r and σ) [42] were employed to maintain the simulation accuracy throughout the broad operational bandwidth of interest including marked increment in conductivity near the resonance frequencies at 3.5, 5.64, 8.4, and 12.9 GHz respectively contributing to reflection loss suppression.

In the electromagnetic simulations, graphene was modeled as a homogeneous conductive material with an electrical conductivity of 4.02×10^5 S/m, corresponding to experimentally reported values for printed graphene conductors used in wearable applications. This conductivity value was assigned in the material definition of the full-wave solver and was consistently applied in all software-based verifications, including reflection coefficient, radiation characteristics, MIMO performance, and SAR analysis.

The obtained conductivity of the graphene antenna illustrates the high quality of graphene layers. This value is much higher than that of common graphene inks (10^2–10^4 S/m) and competitive with commercially available high-conductivity graphene films (typically 10^5–10^6 S/m). This level of conductivity is sufficiently high to provide good radiation efficiency and low ohmic loss at microwave frequencies (3.5 GHz (lower) to 14.4 GHz (higher)) for the planned experiment.

The graphene MIMO antenna conductivity can be expressed by the following equation[25]:

$$\sigma = \frac{L}{R.(W.t)} \tag{2}$$

The parameters in this equation are defined as follows:

- σ (Sigma): Bulk electrical conductivity of the graphene layer, measured in Siemens per meter (S/m) or Siemens per centimeter (S/cm).
- L (length): The length of the conductive graphene sample, which was 1.5 cm in this experiment.
- R (resistance): The measured electrical resistance of the graphene layer was 1.813.
- W (width): The width of the conductive graphene sample is 0.5 cm.
- t (thickness): The thickness of the graphene layer, measured in cm (equivalent to 4.11 m).

SAR distribution and results analysis

The distribution pattern of SAR was evaluated to observe how electromagnetic energy is absorbed by the human phantom at four different resonance frequencies that are reflected in the heat maps presented in Figs. 4(c)–4(f). At the lower-frequency bands of 3.5 GHz and 5.64 GHz, SAR field is already focused at the antenna position on chest with localized "hot spot which decays away into deeper muscle tissues but maintaining maximum SAR values well below safe limit can be seen. As frequency continues to the high-frequency bands, i.e., 8.4 GHz and

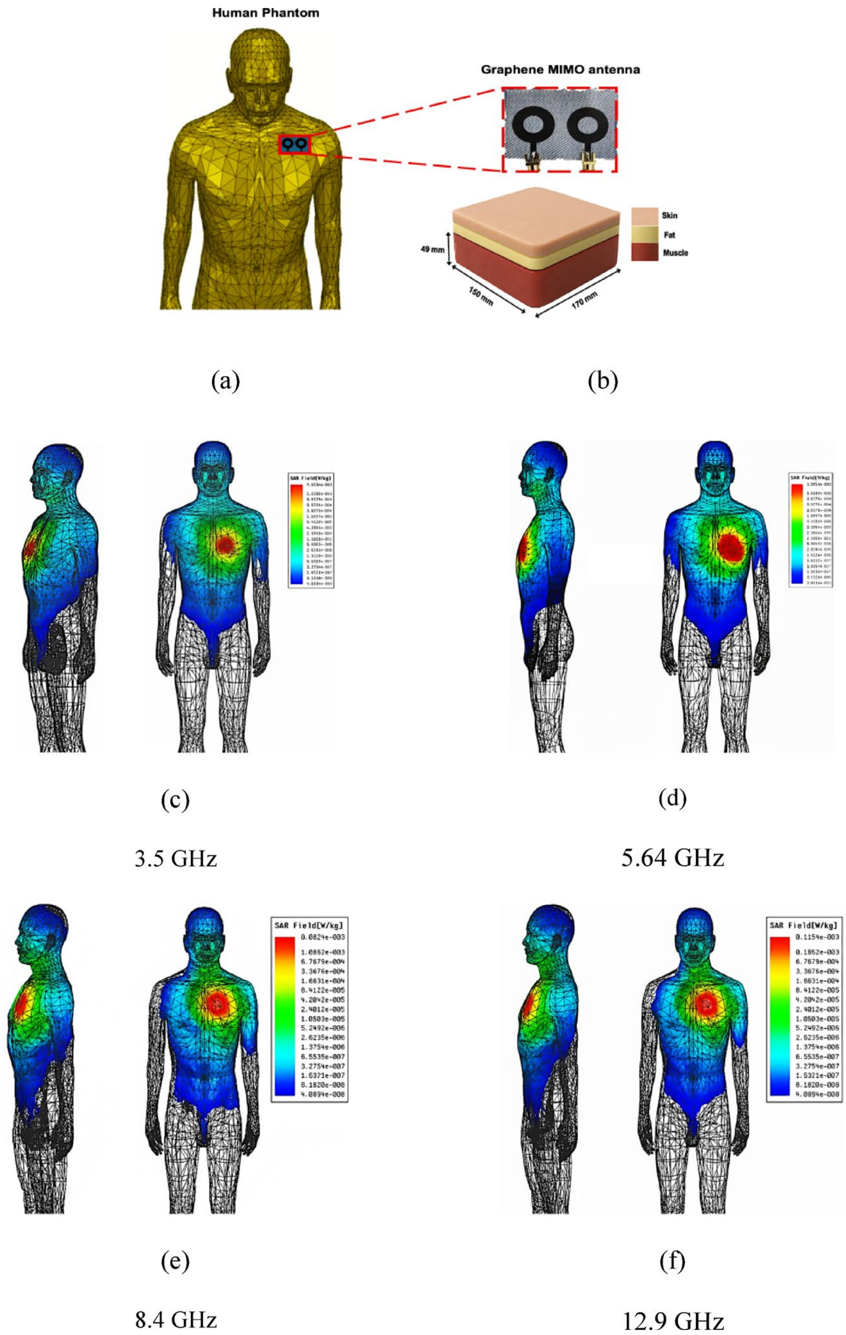

Fig. 4. SAR analysis and modeling: **(a)** 3D human phantom antenna placement; **(b)** Multilayer flat phantom dimensions and Table 2 showing frequency-dependent tissue properties; **(c–f)** SAR field distribution heat maps at 3.5 GHz, 5.64 GHz, 8.4 GHz, and 12.9 GHz, respectively.

Tissue Type	Parameter	3.5 GHz	5.64 GHz	8.4 GHz	12.9 GHz
Skin	Permittivity (ε_r)	37.1	35.5	31.8	30.2
	Conductivity (σ, S/m)	2.85	3.92	8.45	10.15
Fat	Permittivity (ε_r)	5.15	4.95	4.45	4.28
	Conductivity (σ, S/m)	0.18	0.28	0.65	0.82
Muscle	Permittivity (ε_r)	51.8	48.5	42.1	39.5
	Conductivity (σ, S/m)	3.12	4.85	10.95	13.40

Table 2. Dielectric properties of human tissues at operating frequencies.

12.9 GHz, energy absorption becomes quite restricted on only the shallow part of the phantom. This is in line with the frequency-dependent dielectric properties (Table 2), where a relatively higher conductivity at higher frequencies permits less penetration into the body.

Despite these variations in the distribution, the antenna was positioned with a minimal air gap in all simulated cases to replicate realistic on-body placement, and the resulting peak SAR values remained below the international exposure thresholds. This confirms that the graphene-based MIMO design is highly suitable for long-term wearable applications without posing any health risks to the user.

Measured graphene antenna on a human chest body

The on-body performance of the proposed graphene-based MIMO wearable antenna was experimentally evaluated by placing the antenna on a human chest, thereby emulating realistic wearable operating conditions. As illustrated in Fig. 5(a), the measured S_{11} response under free-space conditions shows good agreement with the simulated results. When the antenna is positioned on the human chest, a slight resonance shift and minor impedance variation are observed, which can be attributed to the electromagnetic loading effect of human tissues. Despite this interaction, the antenna maintains $|S_{11}|$ below – 10 dB across the targeted 5G sub-6 GHz operating

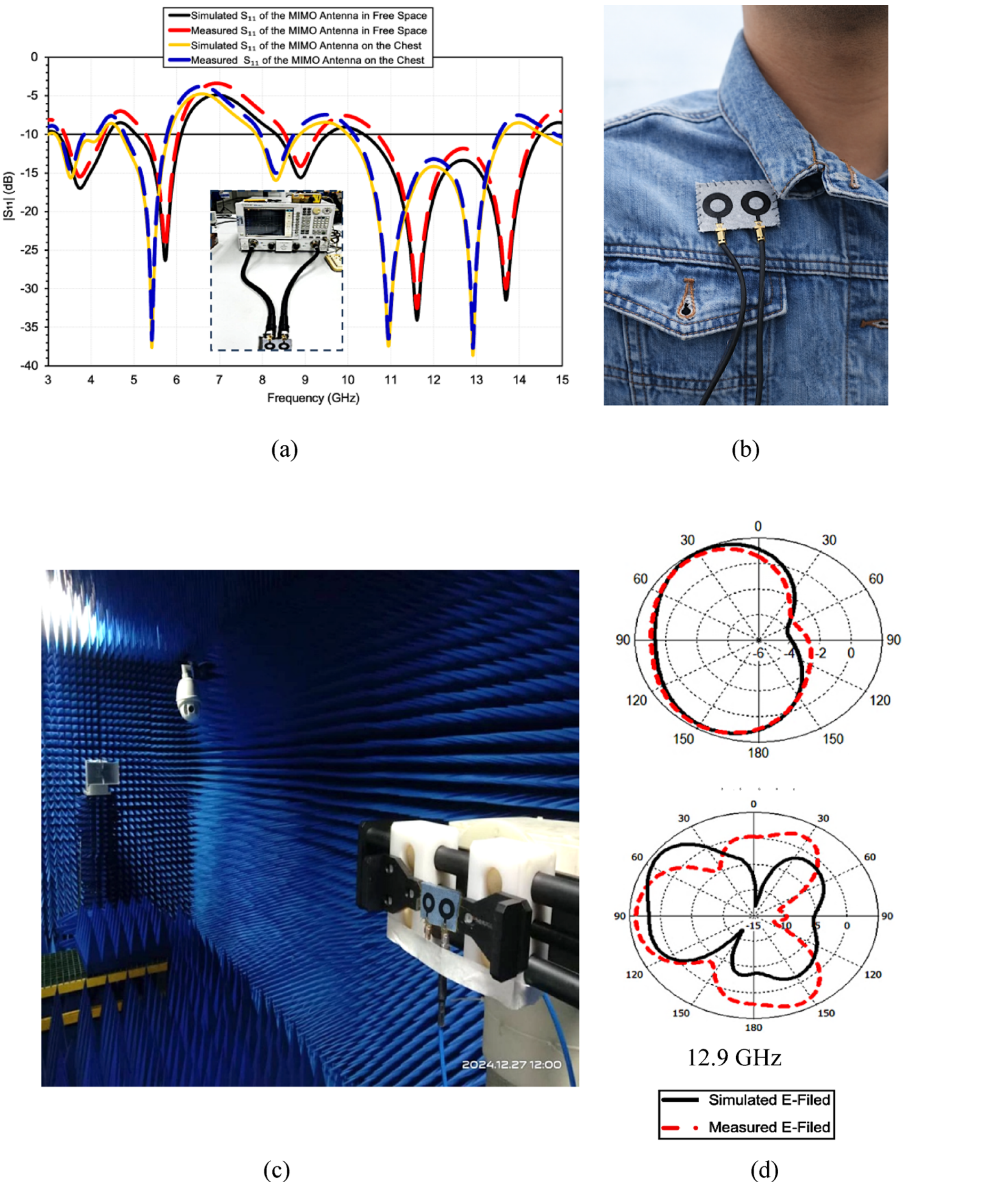

Fig. 5. Measured and simulated performance of the proposed graphene-based wearable MIMO antenna: **(a)** comparison of $|S_{11}|$ under free-space and on-human-chest conditions, including the measurement setup; **(b)** on-body chest measurement photograph; **(c)** anechoic-chamber radiation-pattern measurement setup; and **(d)** comparison of simulated and measured E-plane radiation patterns at 3.5 GHz, and 12.9 GHz.

Ref.	Antenna/Key idea	Size (mm³)	Operational band(s) (GHz)	Peak gain (dBi)	SAR (W/kg) & averaging	Conductor material	Substrate material	On-body/tested location
26	MWCNT-PDMS/PDMS bendable MIMO (vehicular/Wi-Fi)	35 × 70× 2.5	5.78–6.28	4.71 at 5.95 GHz	0.04 W/Kg and 0.05 W/Kg	MWCNT-PDMS ($\sigma \approx 10^5$ S/m)	PDMS ($\varepsilon_r = 2.77$, $\tan\delta = 0.012$, t = 2.5 mm)	Chest, MIMO car model
27	Triangular-slotted UWB flexible antenna (healthcare/breast)	52.6 × 46.3× 1(Jeans)	2.95–24.2	3.16 at 5.8 GHz	0.712 (Flat), 0.152 (Breast)	Copper	Jeans ($\varepsilon_r \approx 1.7$)	Breast phantom (and flat phantom)
28	Wearable textile antenna (broadband; phantom SAR study)	61 × 61 × 1(Jeans)	2.36–16.76	6.9 at 2.4 GHz	max 0.769 (1 g, at 12.944 GHz); also 0.302 (2.954 GHz), 0.594 (5 GHz), etc.	Copper	Jeans	Not reported
29	All-textile broadband MIMO (telecom/medical bands)	54 × 36 × 2.5	1.1–8.6	7.5 at 5.5 GHz (average measured)	Not reported	Graphene	Standard felt ($\varepsilon_r = 1.3$) + cotton fabric ($\varepsilon_r = 2.23$, t = 0.5 mm)	Not reported
30	Star-shaped MIMO on jeans with band-notch (UWB/WLAN)	21 × 16 × 1	2.4–2.485, 5.15–5.825	3.75 at 10.6 GHz	< 1 (1 g, at 10.6 GHz)	Copper	Jeans ($\varepsilon_r = 1.6$)	Wrist placement (explicitly stated)
31	Irregular-octagon 2-port jeans MIMO (sub-6 mid-band)	40 × 50	4.35–7.0 (measured); (simulated) 3.6–7.0	6.5 at 7 GHz	1.93	Copper	Jeans textile	On-body vs. off-body discussed (location NR)
This work	**Graphene 2-port MIMO on jeans (multiband 5Gsub-6, x-band)**	**35 × 55 × 0.5**	**3.1–4.3, 4.9–6.9, 8.25–9.4, 10.28–14.4**	**10.01 at 7.3 GHz**	**0.84 (10 g, 0.5 W)**	**Graphene ($\sigma = 4.02 \times 10^5$ S/m)**	**Jeans ($\varepsilon_r = 1.67$)**	**On-body tissue model (chest)**

Table 3. Comparison of proposed graphene MIMO antenna with recent wearable antennas.

bands (3.1–4.3 GHz and 4.9–6.0 GHz), indicating stable impedance matching under on-body conditions. In addition, two higher-frequency bands are observed at 8.25–9.4 GHz and 10.28–14.4 GHz, making the antenna a strong candidate for X-band system applications.

The practical on-body evaluation setup is shown in Fig. 5(b), confirming the realistic chest-mounted configuration of the antenna on a jeans substrate. In addition, the radiation characteristics of the proposed antenna were experimentally validated inside a fully anechoic chamber, as depicted in Fig. 5(c). The measured and simulated normalized E-plane radiation patterns at representative frequencies of 3.5 GHz and 12.9 GHz are compared in Fig. 5(d). At the lower frequency, the antenna exhibits a quasi-omnidirectional radiation pattern, which is desirable for wearable and body-centric communication scenarios. At the higher frequency, moderate pattern distortion is observed due to the increased electrical size of the antenna and excitation of higher-order resonant modes. Nevertheless, a good overall agreement between simulated and measured radiation patterns is achieved.

A comparative analysis between the proposed graphene-based two-port MIMO antenna and recent wearable antenna designs is presented in Table 3. As shown, many existing wearable antennas focus on either wideband operation or single-/dual-band performance using conventional metallic or composite conductive materials. For example, MWCNT–PDMS-based MIMO antennas reported in[26] demonstrate mechanical flexibility and acceptable gain; however, their operation is limited to a narrow frequency range around the Wi-Fi/WLAN band, and the overall antenna thickness is relatively large due to the PDMS substrate. Other textile-based designs employing copper conductors on jeans substrates[27,28,30,31] provide broadband or dual-band characteristics, but often lack controlled multiband behavior specifically targeting the 5G sub-6 GHz spectrum, and in several cases SAR or detailed on-body placement information is not comprehensively reported.

In contrast, the proposed antenna achieves well-defined multiband operation, simultaneously covering the 5G sub-6 GHz bands (3.1–4.3 GHz and 4.9–6.0 GHz) as well as a higher-frequency X-band (8.25–9.4) and (10.28–14.4 GHz), within a compact footprint of 35 × 55 × 0.5 mm³. Moreover, unlike copper-based wearable antennas, the use of graphene as the radiating material offers advantages in terms of flexibility, durability, and environmental sustainability, while maintaining competitive peak gain performance. Importantly, the proposed design demonstrates SAR compliance under on-body conditions, with a maximum SAR of 0.84 W/kg averaged over 10 g of tissue at 0.5 W input power, which is well below international safety limits. The inclusion of explicit on-body evaluation (chest tissue model) further strengthens the practical relevance of the proposed antenna compared with several prior works summarized in Table 3.

Conclusions

This paper presents the design, fabrication, and experimental validation of a graphene-based two-port MIMO antenna for smart multiband 5G wearable communication applications. With reference to the use of graphene as a radiating material and jeans textile as a substrate, we found that the proposed antenna offers a compact, flexible, and inexpensive clinched solution without degrading the relevant electrical performance. The antenna is multi-band operated in 5G sub-6 GHz range of 3.1–4.9 and 4.9–6.0 GHz with further higher order resonant modes to the extent of 14.4 GHz, thus proving its inherent multi-resonating and wideband performance limitlessness nature. The measured results matched well with the simulation results in air and on the human body, indicating good impedance matching and radiation performance when attached to the chest of a subject. The measurement of the radiation pattern also confirmed that it operated uniformly over both the low- and high-frequency bands. A full SAR analysis verified that the peak energy absorption was significantly (commensurate with tissues) below the ICNIRP safety limits, making it more localized at increasing frequencies to the superficial skin layers, proving the practical functionality of this antenna in long-term wearable systems. In general, the proposed graphene-based MIMO antenna is a potential candidate for future wearable 5G, body centric wireless, and smart wearable communications.

Data availability

The datasets used and/or analysed during the current study available from the corresponding author on reasonable request.

Received: 13 January 2026; Accepted: 27 February 2026
Published online: 04 April 2026

References

1. Al-Gburi, A. J. A., Do We Really Need Frequency-Selective Surface and Metasurface Reflectors for Antenna Gain Enhancement, or Are Metallic Reflectors Enough?, International Journal of Antennas and Propagation, 2026, 2141943, 19 pages, 2026. https://doi.org/10.1155/ijap/2141943.
2. Maheswari, Y., Uma & Roy, B. Design of a flexible compact insensitive wearable antenna for enhanced performance stability. *AEU-International J. Electron. Communications* : 156143. (2025).
3. Omar, M. F. et al. Antenna performances based on distinctive thickness-dependent of flexible substrates: A comprehensive review. *Ain Shams Eng. J.* **16**, 103417 (2025).
4. Al-Gburi, A. J. et al. SAR flexible antenna advancements: highly conductive polymer-graphene oxide-silver nanocomposites. *Progress Electromagnet. Res. M*. **127**, 23–30 (2024).
5 Khattak, R. Y. et al. Design and Performance Investigation of an Ultra-Thin and Flexible Polyimide-Based UWB Antenna. *Results Engineering* : 105956. (2025).
6. Yahya, M.S., Musa, U., Zidan, M.S. et al. Machine learning-optimized compact dual-band medical syringe-inspired wearable antenna for efficient WBAN applications. Sci Rep 15, 43240 (2025). https://doi.org/10.1038/s41598-025-27227-y.
7. Al-Gburi, A. J. A. et al. Electrical conductivity and morphological observation of hybrid filler: Silver-graphene oxide nanocomposites for wearable antenna. *Opt. Mater.* **148**, 114882 (2024).
8. Zhang, J. et al. Ultra-flexible graphene-metal nanomembrane for wireless applications. *npj Flex. Electron.* **9** (1), 27 (2025).
9. Lacour, S. et al. Stretchable gold conductors on elastomeric substrates. *Appl. Phys. Lett.* **82** (15), 2404–2406 (2003).
10. Lu, N. et al. Metal films on polymer substrates stretched beyond 50%. *Appl. Phys. Lett.* **91**, 22 (2007).
11. Sun, Jiancheng, C., Zhang & Zhang, R. Flexible, ultra-low dielectric polyimide aerogels prepared via 10-minute ambient pressure blow-drying for high-gain Sub-6 GHz patch antenna. *Chemical Eng. Journal* : 165571. (2025).
12. Rogers, J., Lagally, M. & Nuzzo, R. Synthesis, assembly and applications of semiconductor nanomembranes. Nature 477, 45–53 (2011). https://doi.org/10.1038/nature10381.
13. Ibanez-Labiano, I. et al. Graphene-based soft wearable antennas. *Appl. Mater. Today*. **20**, 100727 (2020).
14. Sindhu, B. et al. Laser-induced graphene printed wearable flexible antenna-based strain sensor for wireless human motion monitoring. *IEEE Trans. Electron. Devices*. **68**, 3189–3194 (2021).
15. Liu, G. et al. Graphene-assisted metal transfer printing for wafer-scale integration of metal electrodes and two-dimensional materials. *Nat. Electron.* **5** (5), 275–280 (2022).
16. Zhou, X. et al. A sustainable approach towards printed graphene ink for wireless RFID sensing applications. *Carbon*218 : 118693. (2024).
17. Ibanez-Labiano, I. et al. Graphene-based soft wearable antennas. *Appl. Mater. Today*. **20**, 100727 (2020).
18. Douhi, S. et al. Design, characterization, and electromagnetic performance of a flexible wideband RF antenna using composite materials. *J. Science: Adv. Mater. Devices.* **10** (1), 100847 (2025).
19. Gil, I. & Raúl Fernández-García Wearable PIFA antenna implemented on jean substrate for wireless body area network. *J. Electromagn. Waves Appl.* **31**, 11–12 (2017).
20. Mulkalla, S., Fakirde, A. & Paritosh, D. Peshwe. Flexible microstrip patch antenna design on jeans substrate radiating at 2.45 GHz for WBAN application. *Prog Electromagn. Res. M*. **122**, 1–9 (2023).
21. Shyni, G. et al. Simulation and Characterization of Novel Right Scalene Wearable Bowtie Jean Textile Antenna for Wireless Medical Communications. *Braz. J. Phys.* **55** (4), 185 (2025).
22. Avşar Aydın, E. 3D-printed graphene-based bow-tie microstrip antenna design and analysis for ultra-wideband applications. *Polymers* **13**(21), 3724. (2021).
23. Chen, P. et al. Design of UWB wearable conformal antenna based on jean material. *Int. J. Antennas Propag.* **2022**(1), 4886844. (2022).
24. Karad, K. V. et al. A SAR analysis of hexagonal-shaped UWB antenna for healthcare applications. *J Wireless Com Network* **2024**(72), (2024). https://doi.org/10.1186/s13638-024-02405-0
25. Al-Gburi, A. J. et al. Superconductive and flexible antenna based on a tri-nanocomposite of graphene nanoplatelets, silver, and copper for wearable electronic devices. *J. Science: Adv. Mater. Devices*. **9.3**, 100773 (2024).
26. Hussain, M. et al. Design and characterization of multiwall carbon nanotube/polydimethylsiloxane composite MIMO antenna for wearable and vehicular applications. *Sci. Rep.* **15**, 27925. https://doi.org/10.1038/s41598-025-13112-1 (2025).
27. Singh, A. et al. Modeling and simulation of an effectual triangular slotted UWB flexible antenna for breast cancer detection and healthcare monitoring. *PLOS ONE*. **20** (4), e0320806. https://doi.org/10.1371/journal.pone.0320806 (2025).
28. Dwivedi, R., Srivastava, D. K. & Singh, V. K. Innovative wearable textile antenna for holistic prognostic medical applications and perpetual vital signs surveillance of human physiology. *Opt. Quant. Electron.* **57**, 136. https://doi.org/10.1007/s11082-025-08040-3 (2025).
29. Khajeh-Khalili, F. A broadband all-textile wearable MIMO antenna for wireless telecommunication/medical applications. *J. Text. Inst.* **112** (12), 2013–2020. https://doi.org/10.1080/00405000.2020.1862492 (2021).
30. Biswas, A. K., Basu, B., Nandi, A. & Compact Wearable UWB MIMO Antenna with Reduced Mutual Coupling and Notch Characteristics of WLAN Band. *Arab. J. Sci. Eng.* **47**, 14561–14569. https://doi.org/10.1007/s13369-022-06861-y (2022).
31. Pradeep, P., Basha, M. M., Gundala, S. & Syed, J. Development of Wearable Textile MIMO Antenna for Sub-6 GHz Band New Radio 5G Applications. *Micromachines* **15**, 651. https://doi.org/10.3390/mi15050651 (2024).

Acknowledgements

The authors would like to thank Universiti Teknikal Malaysia Melaka (UTeM) and the Ministry of Higher Education (MOHE) of Malaysia for supporting this project.

Author contributions

A.J.A. Al-Gburi conceived the research idea, led the antenna design and development, supervised the overall study, and prepared the original manuscript draft. N.J. Mohammed contributed to the antenna modeling, simulation, fabrication, and experimental validation. Tale Saeidi assisted in performance analysis, MIMO diversity evaluation, and interpretation of the measured results. Nurhayati Nurhayati contributed to the wearable material characterization and supported the SAR analysis and safety assessment. M.M. Ismail provided technical guidance, critically reviewed the manuscript, and contributed to refining the methodology and discussion. All authors reviewed and approved the final manuscript.

Funding

The authors express their sincere gratitude to Universiti Teknikal Malaysia Melaka (UTeM) and the Ministry of Higher Education (MOHE) of Malaysia for their valuable support and funding of this project.Additionally, part of the project was supported by the international grant number ANTARABANGSA (URMG)-USU/2024/FTKEK/A0063.

Declarations

Competing interests

The authors declare no competing interests.

Additional information

Supplementary Information The online version contains supplementary material available at https://doi.org/10.1038/s41598-026-42793-5.

Correspondence and requests for materials should be addressed to N.J.M. or M.M.I.